



**HAL**  
open science

# Contribution of state modelling in efficient MAP symbol-by-symbol demodulation schemes for CPM-MIMO systems

Rim Amara-Boujemâa, Sylvie Marcos

► **To cite this version:**

Rim Amara-Boujemâa, Sylvie Marcos. Contribution of state modelling in efficient MAP symbol-by-symbol demodulation schemes for CPM-MIMO systems. *Signal Processing*, 2014, 96, pp.420-432. 10.1016/j.sigpro.2013.10.006 . hal-01102332

**HAL Id: hal-01102332**

**<https://centralesupelec.hal.science/hal-01102332>**

Submitted on 3 Mar 2020

**HAL** is a multi-disciplinary open access archive for the deposit and dissemination of scientific research documents, whether they are published or not. The documents may come from teaching and research institutions in France or abroad, or from public or private research centers.

L'archive ouverte pluridisciplinaire **HAL**, est destinée au dépôt et à la diffusion de documents scientifiques de niveau recherche, publiés ou non, émanant des établissements d'enseignement et de recherche français ou étrangers, des laboratoires publics ou privés.

# Contribution of state modelling in efficient MAP symbol-by-symbol demodulation schemes for CPM MIMO systems

R. Amara Boujemâa <sup>(1),(2)</sup>, S. Marcos<sup>(3)</sup>

<sup>(1)</sup> *Signals and Systems Unit, National Engineering School of Tunis, B.P 37, Belvédère, Tunis El Manar university, Tunisia*

<sup>(2)</sup> *National Institute of Applied Sciences and Technology, Centre urbain nord, Carthage University, Tunisia*

<sup>(3)</sup> *Signals and systems laboratory, CNRS-supélec, Plateau du Moulon, Gif-Sur-Yvette, France*

*Email : amararim@yahoo.fr / rim.amara@insat.rnu.tn , Sylvie.Marcos@lss.supelec.fr  
Phone : 00.216.1.75.18.14 , 00.33.1.69.85.17.29*

---

## Abstract

In [1], a state model was derived for the demodulation of Continuous Phase Modulation (CPM) signals ; based on which the demodulation problem was solved through the symbol-by-symbol Bayesian estimation built around the MAP Symbol-by-symbol Detector (MAPSD). In this paper, a new state model considered in the augmented state composed of the symbol state and the phase state is proposed and the corresponding modified MAPSD demodulation scheme is presented. The main contribution of the paper however consists in deriving several optimal symbol-by-symbol MAP detection schemes for MIMO systems operating with CPM signals. For this, a state model description of the corresponding demodulation problem is introduced. Based on this state model, two CPM-MIMO Bayesian demodulators are proposed. The first one uses a Zero-Forcing pre-processing block to separate the different CPM signals followed by a bank of MAPSD based CPM demodulators. The second demodulator consists in a joint Decision Feedback (DF) CPM-MIMO MAPSD detector. Simulations confirm the good performance in term

of BER of both proposed structures. Particularly, high BER's performance of the partially joint CPM-MIMO-MAPSD/DF are recorded and an emphasis is made on the implementation simplicity of this new detector with no constraint on the modulation index or the alphabet size.

*Keywords:*

Continuous Phase Modulation, Maximum A Posteriori Bayesian estimation/detection, state model, optimal Bayes filtering , Multi-Input Multi-Output system

---

## **1. Introduction**

The CPM modulation technique offers significant advantages in terms of spectral efficiency and robustness to nonlinearities compared to linear digital modulation techniques. Thereby, CPM is used in GSM, bluetooth and other commercial and military wireless systems [3]. The constant envelope property of CPM signals makes them adequate for more recent applications such as future aeronautical telemetry as suggested in [4] ; where SC-FDMA multiple access technique is used to vehicle based-band CPM samples to reduce the peak-to-average power ratio. Referring to the performance of CPM systems, this last depends strongly on the parameters controlling the modulated signals as well as on the decoding algorithms used to recover the transmitted symbols [2]. Indeed, highly efficient CPM schemes are obtained by introducing memory in the modulation operation which makes the CPM demodulation task more complex. Thus, CPM modulation can be considered as a channel coding technique which can be concatenated with convolutional codes [29] or with irregular repeat accumulate codes [30] to achieve even lower BER performance.

To take advantage of this spectral efficiency induced by the modulation memory, several optimal CPM demodulation/equalization techniques can be employed [2]. Optimal CPM demodulation algorithms, which is the problematic treated in this work, rely gen-

erally on Maximum Likelihood Sequence estimation (MLSD) schemes implemented with the computationally efficient Viterbi algorithm [5]-[10]. Among such MLSD based solutions, many demodulation algorithms are derived using the Laurent representation of binary CPM signals and the resulting demodulator is then structured into a bank of matched filters followed by a Viterbi module search. This structure is also used to deal with multi-user [9] or cochannel CPM signal detection [8]. Generally, the complexity of MLSD-based CPM decoders grows for longer partial response lengths or for high modulation alphabet size. Consequently, several suboptimal ML CPM demodulation algorithms were derived, in order to reduce the complexity of the required algorithms, by approximating or truncating the Laurent expansion [9][16]. Dimensionality reduction of CPM signal representations was also treated in [28] using the principle component analysis.

On the other hand, many other optimal Bayesian CPM demodulators designed to minimize the achieved symbol error probability provide the Maximum *A Posteriori* (MAP) symbol estimates instead of the ML ones. In [10], MLSD detection is replaced by a MAP Sequence Detector implemented using the forward/backward recursions. In some similar works, MAP symbol-by-symbol demodulation is preferred when soft output metrics are to be used to enhance the receiver performance [10]-[14]. In this paper, the problem of CPM demodulation is also considered within a MAP symbol-by-symbol detection framework by proposing a state representation of the demodulation problem as introduced in our earlier work [1]. Particularly, we focus on extending the idea of state modelling to coherent demodulation of CPM signals included within a MIMO system. Consequently, once a state representation is given, CPM demodulation can be handled through powerful nonlinear optimal estimation tools such as methods based on parallel Kalman filtering, particle filtering ...etc.

Indeed, CPM modulation are shown to provide high data rates performance when used in multi-antennas systems [15]. Several CPM-MIMO receivers based whether on MLSD

joint symbol sequence detection and the Laurent representation [16] or on the blind signal separation at the front-end of a frequency discriminator based CPM demodulator [17] are detailed in the corresponding references. In this work, a state model, considered in the transmitted data streams and describing the joint demodulation problem within a CPM-MIMO system is derived by up-sampling the mixture of the different CPM modulated signals. The state model turning out to be non gaussian and nonlinear, this suggests eventually the application of a panoply of optimal nonlinear estimators [18][19] to decode the CPM signals. In fact, the contribution of state modelling of several digital communication problems, allowing the use of subsequent optimal filters has been shown to offer near optimal performance in many applications [20][21]. For example, in [23][24], Collings *et al.* use state modelling to develop a Kalman/HMM filter for phase modulated signals in unknown noisy fading channels. Here also, we give an approach to the problem of CPM-MIMO demodulation based on state estimation. As the state to estimate in our derived CPM-MIMO state model is finite-value, the well-known Bayes filtering equations, for optimal filtering, can be implemented, without approximation, to deal with the MAP CPM symbol detection as done in [22]. As the observation vector at the demodulator output is related to the phase states corresponding to the different entries, a Decision Feedback (DF) mechanism is integrated then into the MAPSD-based detection scheme when dealing the joint demodulation of these entries mixed via the MIMO channel. So, to recapitulate, compared to previous works on Bayesian CPM demodulation, our contributions are :

- developing reduced complexity MAP symbol-by-symbol detectors
- MAP symbol-by-symbol demodulation of CPM-MIMO signals hasn't been treated before, which is the main novelty of the paper
- The proposed MAPSD schemes for CPM demodulation don't need a fractional value of the modulation index and are applicable for any modulation alphabet
- In the available literature on MAP symbol-by-symbol Bayesian CPM demodulation, and

here we cite precisely the works of Balasubramanian *et al.*[13], of Gertsman *et al.*[11] and of Abend and Fritchmann[2], the corresponding CPM Bayesian demodulation algorithms are used to determine recursively the infinite horizon conditional *a posteriori* symbol pdf through marginalization and using the Bayes rule ; but in different ways, at different stages and hence with different layouts. In this paper, the symbol pdf derivation that is used follows directly from the Bayes filtering equations running in two stages, namely the prediction and the filtering or updating steps [18][19].

So, above all these advantages, formulating the CPM demodulation, whether in the SISO or MIMO case, as a state representation accommodates the demodulation problem and the problem of estimation of all the related parameters characterizing the receiver input to a variety of nonlinear Bayesian estimation tools, that have been extensively studied in the literature and has been shown to perform optimally

The paper is organized as follows. Section 2 recalls the different state models derived to deal with the CPM demodulation problem in additive white gaussian noise context. Particularly, a new state model including the symbol state and the CPM phase state term is proposed. Section 3 explicits the different MAP symbol-by-symbol detection schemes corresponding to the so-derived state models and based on the MAPSD detection algorithm. In section 4, the state model for the CPM-MIMO demodulation is derived. Sections 5 and 6 detail then the proposed alternatives for the CPM-MIMO MAP symbol-by-symbol demodulation and their principles. Section 7 presents the simulation results and section 8 gives the conclusion.

*Notations.*  $(.)^*$  denotes the complex conjugate operator,  $\propto$  the proportionality operator. Vectors are typed in bold characters. If  $\mathbf{x} = [x_1, x_2, \dots, x_n]^T$  is a column vector of length  $n$ , then we denote by  $\mathbf{x}[i : j] = [x_i, x_{i+1}, \dots, x_j]^T$  and  $\mathbf{x}[i] = x_i$  the  $i^{th}$  component of  $\mathbf{x}$ . If

$\mathbf{x}_1, \dots, \mathbf{x}_n$  is a collection of  $n$  column vectors, then  $\text{vec}(\mathbf{x}_{i=1}^n) = [\mathbf{x}_1^T \dots \mathbf{x}_n^T]^T$ . When  $\mathbf{x}$  is a vector  $n \times 1$  then  $e^{\mathbf{x}} = [e^{x_1}, e^{x_2}, \dots, e^{x_n}]^T$ . A gaussian variable  $x$  is designed by  $\mathcal{N}(m_x, \sigma_x^2)$  with mean  $m_x = E\{x\}$  and variance  $\sigma_x^2 = E\{x^2\} - |m_x|^2$ .  $I_M$  is the identity matrix of dimension  $M \times M$ . We denote by  $F_L$  the one step transition matrix of dimension  $L \times L$  and given by

$$F_L = \begin{bmatrix} 0 & 0 & 0 & \dots & 0 \\ 1 & 0 & 0 & \dots & 0 \\ 0 & 1 & 0 & \dots & 0 \\ \dots & \dots & \dots & \dots & \dots \\ 0 & \dots & 0 & 1 & 0 \end{bmatrix} \text{ and } \mathbf{G}_L = \begin{bmatrix} 1 \\ 0 \\ \vdots \\ 0 \end{bmatrix} \text{ of length } L$$

$\odot$  denotes the Shur product and  $\otimes$  denotes the Kronecker product. If  $\mathbf{x}(n)$  denotes a stochastic process, we design the filtration  $\{\mathbf{x}(k), \dots, \mathbf{x}(k')\}$  by  $\mathbf{x}_{k:k'}$ .

## 2. State formulation of the CPM demodulation problem

The complex envelope of a CPM modulated signal is given by [2]

$$r_c(t) = \sqrt{\frac{2E_s}{T_s}} e^{j\phi(t;d)}$$

where  $T_s$  denotes the symbol period,  $E_s$  is the transmitted energy per symbol and  $\phi(t; d)$  is the instantaneous CPM angle related to the shaping filter output by

$$\phi(t; d) = 2\pi h \int_0^t \sum_n d(n)g(u - nT_s)du \quad \text{for } t \geq 0 \quad (1)$$

$d(n) \in \Delta = \{\pm 1, \pm 3, \dots, \pm(K - 1)\} = \{\delta_i, 1 \leq i \leq K\}$  denotes actually the transmitted symbol at the  $n^{\text{th}}$  signalling period laying in the modulation alphabet  $\Delta$ ,  $h$  is the modulation index and  $g(t)$  is the impulse response of the shaping filter which is nonzero in the interval  $[0, LT_s]$ . The CPM modulation is said to be full-response if  $L = 1$  and of partial response

if  $L > 1$ . Over the  $k^{\text{th}}$  symbol period  $[kT_s, (k+1)T_s]$ , the instantaneous CPM signal phase can then be written as

$$\phi(t; d) = \underbrace{\pi h \sum_{n=-\infty}^{k-L} d(n)}_{\theta_k} + \underbrace{2\pi h \sum_{n=k-L+1}^k d(n)q(t-nT_s)}_{\theta(t; d)} \quad (2)$$

where  $q(t) = \int_0^t g(u)du$  is the phase smoothing response such that  $q(t) = 1/2 \forall t \geq LT_s$ .

The CPM signal phase  $\theta(t; d)$  can then be synchronously oversampled at  $T_e = \frac{T_s}{M}$  ( $M$  denotes actually the oversampling factor), leading to

$$\begin{aligned} \theta(kT_s + mT_e; d) &= 2\pi h \sum_{n=k-L+1}^k d(n)q(kT_s + mT_e - nT_s) \\ &= 2\pi h \sum_{n=0}^{L-1} d(k-n)q(nT_s + mT_e) \\ &= 2\pi h \mathbf{q}_m^T \mathbf{D}_L(k) \quad \text{for } 0 \leq m \leq M-1 \end{aligned}$$

where  $\mathbf{q}_m = [q(mT_e) \ q(mT_e + T_s) \ \dots \ q(mT_e + (L-1)T_s)]^T$  and  $\mathbf{D}_L(k) = [d(k) \ d(k-1) \ \dots \ d(k-L+1)]^T$  is designed hereafter by the  $L$ -length symbol state. Consequently, we form the vector of the  $M$  phase samples as follows

$$\begin{aligned} \Phi(k) &= [\phi(kT_s; d) \ \phi(kT_s + T_e; d) \ \dots \ \phi(kT_s + (M-1)T_e; d)]^T \\ &= \theta_k \mathbf{1}_M + \Theta(k) \quad \text{with} \quad \Theta(k) = 2\pi h Q \mathbf{D}_L(k), \end{aligned}$$

where  $\mathbf{1}_M = [1, \dots, 1]^T$  of dimension  $M \times 1$  and  $Q^T = [\mathbf{q}_0, \dots, \mathbf{q}_{M-1}]$ . The problem of CPM demodulation consists then in detecting the transmitted symbol sequence by processing the base-band received noisy CPM samples stacked into one vector over the symbol period  $[kT_s, (k+1)T_s]$  and denoted by

$$\mathbf{r}(k) = \text{vec}(r_c(kT_s + (i-1)T_e) + n_c(kT_s + (i-1)T_e)|_{i=1}^M) = e^{j\Phi(k)} \mathbf{1} + \mathbf{n}(k)$$

---

<sup>1</sup>the factor  $\sqrt{\frac{2E_s}{T_s}}$  is omitted provided that we take account of it when computing the SNR

where  $\mathbf{n}(k) = [n_c(kT_s) \ n_c(kT_s + T_e) \ \dots \ n_c(kT_s + (M - 1)T_e)]^T$  is the vector of the up-sampled time-continuous additive complex white gaussian noise  $\mathcal{N}(0, \sigma_n^2)$ . So, the CPM demodulation problem can be considered within an optimal estimation framework based on the following state model description in the hidden Markov process  $\mathbf{D}_L(k)$

$$\begin{cases} \mathbf{D}_L(k + 1) = F_L \mathbf{D}_L(k) + \mathbf{G}_L d(k + 1) \\ \mathbf{r}(k) = e^{j\theta_k} e^{j2\pi h Q \mathbf{D}_L(k)} + \mathbf{n}(k) \end{cases} \quad (3)$$

### 2.1. State model A

As we can notice, the state transition equation is linear in  $\mathbf{D}_L(k)$  with a discrete finite-value state noise  $\mathbf{G}_L d(k + 1)$  and the observation one is a nonlinear equation, in which a kind of control term is highlighted, which is  $e^{j\theta_k}$ . One way to approximate this term is to generate an estimate of the phase state  $\theta_k$  recursively as with a DF mechanism, according to

$$\hat{\theta}_k = \hat{\theta}_{k-1} + \pi h \hat{d}(k - L) \quad (4)$$

where  $\hat{d}(k - L)$  is the  $L$ -delayed decoded symbol that can be obtained from the previous processing iterations. Besides, the rotated vector  $\mathbf{z}(k) = e^{-j\hat{\theta}_k} \mathbf{r}(k)$  is taken as observation which, under the condition of error-free detected symbols (or limited error propagation), should yield to

$$\begin{cases} \mathbf{D}_L(k + 1) = F_L \mathbf{D}_L(k) + \mathbf{G}_L d(k + 1) & \text{State Model A} \\ \mathbf{z}(k) \simeq \mathbf{f}_L(\mathbf{D}_L(k)) + \mathbf{n}'(k) \end{cases}$$

where  $\mathbf{f}_L(\mathbf{D}_L(k)) = e^{j2\pi h Q \mathbf{D}_L(k)}$ .

### 2.2. State model B

In the second alternative, a discrete differentiation of the observation vector is achieved, as realized in [25], in order to eliminate the contribution of the cumulative term in  $\theta_k$  as

explained below

$$\begin{aligned}
\mathbf{z}(k) &= \mathbf{r}(k) \odot \mathbf{r}^*(k-1) \\
&= e^{j\theta_k} e^{j2\pi h Q \mathbf{D}_L(k)} \odot e^{-j\theta_{k-1}} e^{-j2\pi h Q \mathbf{D}_L(k-1)} + \mathbf{n}''(k) \\
&= e^{j\pi h d(k-L)} e^{j\pi 2h Q(\mathbf{D}_L(k) - \mathbf{D}_L(k-1))} + \mathbf{n}''(k)
\end{aligned} \tag{5}$$

So, if we denote by  $\mathbf{D}_{L+1}(k) = [d(k), d(k-1), \dots, d(k-L)]^T$  the symbol state vector of length  $(L+1)$  to which  $\mathbf{z}(k)$  is related, then, a second state model describing the CPM demodulation problem can be written as

$$\begin{cases} \mathbf{D}_{L+1}(k+1) = F_{L+1} \mathbf{D}_{L+1}(k) + \mathbf{G}_{L+1} d(k+1) & \text{State Model B} \\ \mathbf{z}(k) \simeq \mathbf{f}_{L+1}(\mathbf{D}_{L+1}(k)) + \mathbf{n}''(k) \end{cases}$$

$$\text{where } \mathbf{f}_{L+1}(\mathbf{D}_{L+1}(k)) = e^{j\pi h \mathbf{D}_{L+1}(k)[L+1]} e^{2j\pi h Q(\mathbf{D}_{L+1}(k)[1:L] - \mathbf{D}_{L+1}(k)[2:L+1])}$$

this last derived state formulation is especially appropriate for non coherent CPM symbol detection schemes which may be subject to carrier recovery problems and which are based generally on phase discrimination or differential detection [26]-[27].

### 2.3. State model C

As most of Viterbi based Maximum Likelihood (ML) CPM decoders, a third state model considered in the augmented state  $\mathbf{X}(k) = [\mathbf{D}_L^T(k) \theta_k]^T$  can already be used by writing

$$\begin{cases} \mathbf{X}(k+1) = F' \mathbf{X}(k) + \mathbf{w}(k+1) & \text{State Model C} \\ \mathbf{z}(k) = \mathbf{r}(k) = \mathbf{f}_e(\mathbf{X}(k)) + \mathbf{n}(k) \end{cases}$$

---

<sup>2</sup>corresponds actually to one state of the Viterbi treillis augmented with the symbol  $d(k)$

where  $F' = \begin{bmatrix} F_L & \mathbf{0}_{L \times 1} \\ \mathbf{0}_{1 \times L} & 1 \end{bmatrix}$  and  $\mathbf{w}(k+1) = \begin{bmatrix} \mathbf{G}_L d(k+1) \\ \pi h d(k-L+1) \end{bmatrix}$ .

Here also, the state transition equation is a simple linear shift equation describing the finite-value hidden Markov state formed by the concatenation of  $\mathbf{D}_L(k)$  and  $\theta_k$ ; with a discrete-value state noise vector. In the observation equation, the same nonlinear expression in the augmented state as  $\mathbf{r}(k)$  is kept as well as the same observation noise.

So, based on the proposed state models A, B and C, several Bayesian optimal filters can be applied to derive for example the  $k_0$ -delayed MMSE estimated symbols  $\hat{d}_{MMSE}(k-k_0)$  or the MAP detected ones  $\hat{d}_{MAP}(k-k_0)$ , when a symbol-by-symbol detection mode is adopted. These symbol estimators are to be determined through the computation of the *a posteriori* symbol distribution  $p(d(k-k_0)|\mathbf{z}_{0:k})$  obtained by marginalization of the state conditional probability distribution.

### 3. MAPSD algorithm for CPM demodulation

In this section, we present different schemes for MAP symbol-by-symbol CPM demodulation, based on the MAPSD-algorithm [22] and on the state models introduced in section 2. Let us recall that the MAPSD algorithm consists in fact in a practical matricial implementation of the well-known Bayes filtering equations when the state model takes a finite number of values. When the same symbol detection mode is adopted, the MAPSD detection algorithm should yield to the same MAP symbol decisions made by the Abend and Fritchmann implementation of a MAP symbol-by-symbol detector as detailed in [2].

#### 3.1. Noise statistical characterisation through the derived state models A and B

Examining first the statistics of the noise highlighted in state model A

$$\mathbf{n}'(k) = [n'_1(k), \dots, n'_M(k)]^T = e^{-j\hat{\theta}_k} \mathbf{n}(k)$$

and since the estimated detected symbol tail  $\hat{\theta}_k$  depends statistically on  $\mathbf{z}_{0:k-1}$ ; then given the value of  $\hat{\theta}_k$ , the discrete-time noise process  $\{n'_i(k)\}_{i,k}$  is shown to be well modeled by a gaussian  $\mathcal{N}(0, \sigma_n^2)$  [1]. Further, it is clear that, given  $\mathbf{z}_{0:k-1}$ ,  $\mathbf{n}'(k)$  and  $\mathbf{D}_L(k)$  are uncorrelated which allows subsequent Bayes filtering equations to be hold when determining  $p(\mathbf{D}_L(k)|\mathbf{z}_{0:k})$ . As for state model B, the noise vector is expressed by

$$\mathbf{n}''(k) = \mathbf{n}(k) \odot e^{-j\Phi(k-1)} + \mathbf{n}^*(k-1) \odot e^{j\Phi(k)} + \mathbf{n}(k) \odot \mathbf{n}^*(k-1) = [n''_1(k), \dots, n''_M(k)]^T$$

in [1], it was shown that the discrete-time noise  $\{n''_i(k)\}_{i,k}$  can be modelled by a white gaussian  $\mathcal{N}(0, \sigma_{n''}^2)$  with  $\sigma_{n''}^2 = 2\sigma_n^2 + \sigma_n^4$ .

Table 1 shows actually that the theoretical and sample variances of  $n'_i(k)$  and  $n''_i(k)$  coincide. For example, figure 1 visualizes the superposition of the sample and theoretical pdf of the real and imaginary parts of  $n''(\cdot)$  to confirm the validity of the gaussian assumption.

### 3.2. MAPSD algorithm for CPM demodulation based on state model A and B

So, based on state model A or B, a delayed MAP symbol-by-symbol estimate can be obtained to achieve the demodulation task by taking

$$\hat{d}_{MAP}(k - k_0) = \arg \max_{\delta_i} p(d(k - k_0) = \delta_i | \mathbf{z}_{0:k}) \quad (6)$$

with  $k_0 = L - 1$  if state model A is used and  $k_0 = L$  for state model B. The delayed symbol *a posteriori* pdf is computed by marginalization using

$$p(d(k - k_0) = \delta_i | \mathbf{z}_{0:k}) = \sum_{j | \mathbf{D}_{k_0+1}^j[k_0+1] = \delta_i} p(\mathbf{D}_{k_0+1}(k) = \mathbf{D}_{k_0+1}^j | \mathbf{z}_{0:k}) \quad (7)$$

where  $\mathbf{D}_{k_0+1}^j, j = 1, \dots, N = K^{k_0+1}$  denote all the possible values of the  $(k_0 + 1)$ -length transmitted symbol sequence  $\mathbf{D}_{k_0+1}(k)$ . So, let  $p_j(k) = p(\mathbf{D}_{k_0+1}(k) = \mathbf{D}_{k_0+1}^j | \mathbf{z}_{0:k})$  be the *a posteriori* symbol state probability of the  $j^{\text{th}}$  possible symbol sequence  $\mathbf{D}_{k_0+1}^j$ . Here is the

resume of the MAPSD symbol detection algorithm based on state model A or B and applied to the CPM demodulation problem

Let  $\mathbf{p}(k) = [p_1(k), \dots, p_N(k)]^T$  be the vector of the *A Posteriori* Probabilities (APP) corresponding to all the possible symbol sequences

**1. Initialize  $\mathbf{p}(0)$ <sup>3</sup>**

**2. At iteration  $k$ ,  $\mathbf{p}(k-1)$  and the new observation  $\mathbf{z}(k)$  are available at the MAPSD**

**2.a Prediction step**

Compute the predicted symbol state probabilities according to

$$\mathbf{p}(k|k-1) = A\mathbf{p}(k-1) \quad (8)$$

where  $A$  is the probability transition matrix of the hidden Markov state  $\mathbf{D}_{k_0+1}(k)$  such that

$$A(i, j) = p(\mathbf{D}_{k_0+1}(k) = \mathbf{D}_{k_0+1}^i | \mathbf{D}_{k_0+1}(k-1) = \mathbf{D}_{k_0+1}^j) \quad (9)$$

for i.i.d symbols,  $A$  has null elements except for the couple of indices  $(i, j)$  such that  $\mathbf{D}_{k_0+1}^i[2 : k_0 + 1] = \mathbf{D}_{k_0+1}^j[1 : k_0]$ , for which we have  $A(i, j) = \frac{1}{K}$ .

**2.b Filtering or updating step**

- determine the observation likelihood vector  $\mathbf{p}_n(k)$  such that

$$\mathbf{p}_n(k)[i] \propto \exp \left\{ -\frac{1}{2\sigma_n^2} \|\mathbf{z}(k) - \mathbf{f}_{k_0+1}(\mathbf{D}_{k_0+1}^i)\|^2 \right\} \quad (10)$$

where the notation  $n(\cdot)$  stands for  $n'(\cdot)$  or  $n''(\cdot)$  according to the value of  $k_0$ .

- APP update according to

$$\mathbf{p}(k) = \frac{1}{C_k} \mathbf{p}(k|k-1) \odot \mathbf{p}_n(k) \quad (11)$$

---

<sup>3</sup>if a known preamble is available at the receiver an initialization of  $\mathbf{p}(0)$  to the true value is done

where  $C_k = \mathbf{p}_n^T(k)\mathbf{p}(k|k-1)$  is the APP normalization factor

3. symbol detection according to (7)-(6), then  $k = k + 1$

### 3.3. MAPSD-algorithm based on state model C

The application of the MAPSD-algorithm is also straightforward when the CPM demodulation is described by state model C. In this case, the state vector takes a finite number of values if the modulation index  $h$  is fractional i.e  $h = m/P$  where  $m$  and  $P$  are co-prime positive integers. So that the phase state term  $\theta_k$  lays in

$$\Theta_s = \{0, \frac{\pi m}{P}, \frac{2\pi m}{P}, \dots, \frac{(P-1)\pi m}{P}\} \quad \text{if } m \text{ is even, } \text{card}(\Theta_s) = P$$

and in

$$\Theta_s = \{0, \frac{\pi m}{P}, \frac{2\pi m}{P}, \dots, \frac{(2P-1)\pi m}{P}\} \quad \text{if } m \text{ is odd, } \text{card}(\Theta_s) = 2P$$

Hence the state vector  $\mathbf{X}(k)$  takes  $N = PK^L$  or  $N = 2PK^L$  values according to the parity of  $m$ . Assuming that the state process  $\mathbf{X}(k)$  is homogeneous, the state transition probability is determined as follows

$$\begin{aligned} p(\mathbf{X}(k)|\mathbf{X}(k-1)) &= p(\mathbf{D}_L(k)|\theta_k, \mathbf{D}_L(k-1), \theta_{k-1})p(\theta_k|\mathbf{D}_L(k-1), \theta_{k-1}) \\ &= p(\mathbf{D}_L(k)|\mathbf{D}_L(k-1))p(\theta_k|d(k-L), \theta_{k-1}) \end{aligned}$$

when using the decorrelation of the transmitted symbols. The first distribution indicating the transition probability between the symbol states  $\mathbf{D}_L(k)$  is determined as in (9). The term  $p(\theta_k|d(k-L), \theta_{k-1})$  is a point mass distribution whose value is 1 if and only if the value of  $\theta_k$  coincide with the value of  $\theta_{k-1} + \pi h d(k-L)$  modulo  $2\pi$ . Denoting by  $\theta_s^i$  the elements of  $\Theta_s$  the APP update equation remains the same as in (11) when  $\mathbf{f}_{k_0+1}(\mathbf{D}_{k_0+1}^i)$  is replaced by  $\mathbf{f}_e(\mathbf{X}^i)$  and  $\mathbf{X}^i = [(\mathbf{D}_L^j)^T \ \theta_s^l]^T$  for some  $j \in \{1, \dots, K^L\}$  and  $l \in \{1, \dots, P(\text{ or } 2P)\}$ . Then, the  $(L-1)$ -delayed symbol *a posteriori* pdf is obtained from the APP vector through marginalization over  $\theta_k$  and the remaining symbols in  $\mathbf{D}_L(k)$ .

### 3.4. Complexity features

As most of Bayesian CPM demodulators, including the Viterbi-based MLSE detectors, the complexity of the detection algorithms is expressed in the number of computed metrics per algorithm iteration. Hereafter, the complexity of the different version of the MAPSD-based CPM demodulators versus the one of Viterbi-based ML CPM detector and that of the Optimum Soft Algorithm OSA [13]

for MLSD : Since the treillis state length is  $PK^{L-1}$  or  $2PK^{L-1}$ , then  $P(2P)K^L$  metrics are computed at each iteration, so the complexity is in  $O(P(2P)K^L)$

for OSA : the complexity is in  $O(k_0K^2.K^{L-1})$ , for example, if  $k_0 = L - 1$  then the complexity is in  $O((L - 1)K^{L+1})$

for MAPSD-augmented : the complexity is in  $O(P(2P)K^L)$

for MAPSD-DF : the complexity is in  $O(K^L)$

As we can see, the MAPSD-DF exhibits the lowest complexity order. This complexity is as drastically lower for large values of  $P$ . In fact, as illustrated further in the simulation section, the performance of maximum likelihood detection in terms of BER is improved if the minimum Euclidian distance between two paths .... denoted by  $d_B^2(h)$  in [2] is chosen optimally. Hence, optimal choice of the modulation index  $h$  achieving low values of  $d_B^2(h)$  can be written as a fractional with  $P$  high. In this case, the complexity of MAPSD-augmented and the Viterbi-based CPM decoder becomes much greater than that of the MAPSD-DF

### 3.5. Remarks

- Let us note that the MAPSD is actually a soft symbol-by-symbol detector based on the recursive determination of the infinite horizon *a posteriori* pdf  $p(\mathbf{D}_{k_0+1}(k)|\mathbf{z}_{0:k})$  for  $k_0 = L - 1$  or  $k_0 = L$ . A smoothing-based version for the detection mode can also be brought out as the information on the delayed symbol  $d(k - k_0)$  is also available via the probability

measures  $p(\mathbf{D}_{k_0+1}(k-i)|\mathbf{z}_{0:k-i})$ ,  $i = 1, \dots, k_0$ . Also, the CPM decoding can be processed by using the MMSE (Minimum Mean Square Error) criterion instead of MAP as follows

$$\hat{d}_{MMSE}(k-k_0|k) = \text{dec}\left(\sum_{i=1}^K \delta_i p(d(k-k_0) = \delta_i | \mathbf{y}_{0:k})\right)$$

which becomes, when a  $k_0$ -lag smoothed estimated symbol is to be determined

$$\hat{d}_{MMSE}(k-k_0) = \text{dec}\left(\frac{1}{k_0+1} \sum_{i=0}^{k_0} \hat{d}_{MMSE}(k-k_0|k-i)\right)$$

$\text{dec}(\cdot)$  is the decision function on the symbols. In this work, we focused on the MAP criterion as it guarantees the minimum achievable error probability per symbol.

- The proposed CPM detection schemes corresponding to state models A, B are actually **free constraint towards the choice of the modulation index  $h$  and the alphabet size  $K$** ; compared to ML CPM sequence detectors which require  $h$  to be fractional. Among such detectors, many alternative structures based on the Laurent representation of the CPM signal need binary CPM constellations to be processed.

In the following, when the MAPSD is applied based on state model A, it is referred to the MAPSD with Decision-Feedback (**MAPSD-DF**) version of the symbol-by-symbol CPM demodulation algorithm. When the state model B is adopted through the differentiation of the observation vector  $\mathbf{r}(k)$ , the corresponding detection algorithm is referred to the **MAPSD-differential**. The version of the MAPSD based on state model C is further designed by the **MAPSD-augmented**.

#### 4. CPM-MIMO system description based on state modelling

As it is presented in the previous section, an adequate state formulation can be already established to deal with the CPM demodulation problem by processing an over-sampled

version of the CPM modulator output. Regarding the nonlinear/nongaussian structure of the state model, some performant nonlinear filtering tools can already be suggested. This constitutes then a real motivation for the investigation of the contribution of such state modelling in a general and more complete CPM-MIMO systems. So, let us consider a MIMO system which is depolyed with  $N_t$  transmit and  $N_r$  receive antennas as illustrated by figure 2. The transmitted signals by the  $N_t$  antennas correspond to different CPM modulated signals related to different digital data streams  $d_i(k) \quad i = 1, \dots, N_t$ . The diversity is offered in this context through a known bloc fading channel matrix  $H$  for which, each component  $h_{ij}$  is a flat Rayleigh fading channel coefficient from the  $j^{\text{th}}$  transmit to the  $i^{\text{th}}$  receive antenna. Each  $h_{ij}$  is supposed to be a complex gaussian random variable  $CN(0, 1)$ . The different channels are assumed to be statistically independent.

Denoting by  $r_l(t)$  the CPM signal transmitted by the  $l^{\text{th}}$  antenna, the noisy time-continuous received signal by the  $i^{\text{th}}$  antenna is given by

$$y_i(t) = \sum_{l=1}^{N_t} h_{il}r_l(t) + n_i(t)$$

which, when  $M$ -upsampled over the symbol period  $[kT_s, (k+1)T_s[$  yields to the vector

$$\mathbf{y}_i(k) = \begin{bmatrix} y_i(kT_s) \\ y_i(kT_s + T_e) \\ \vdots \\ y_i(kT_s + (M-1)T_e) \end{bmatrix} = [ (h_{i1} \ h_{i2} \ \dots \ h_{iN_t}) \otimes I_M ] \mathbf{r}(k)$$

where  $\mathbf{r}(k)$  is the concatenation of the  $N_t$  upsampled transmitted CPM signals expressed by the following  $MN_t$ -length vector

$$\mathbf{r}(k) = \text{vec}(\mathbf{r}_i(k)|_{i=1}^{N_t}) \text{ where } \mathbf{r}_i(k) = e^{j\theta_{k,i}} e^{j2\pi h \mathbf{Q} \mathbf{D}_{L,i}(k)}$$

and where, as in the case of the previously presented single data CPM demodulation scheme

$$\theta_{k,i} = \theta_{k-1,i} + \pi h d_i(k - L), \quad i = 1, \dots, N_t$$

$$\mathbf{D}_{L,i}(k+1) = F_L \mathbf{D}_{L,i}(k) + \mathbf{G}_L d_i(k+1) \quad \text{with} \quad \mathbf{D}_{L,i}(k) = [d_i(k), \dots, d_i(k-L+1)]^T$$

Consequently, concatenating the observation vectors  $\mathbf{y}_i(k)$  at the output of the  $N_r$  samplers of the receive antennas over  $[kT_s, (k+1)T_s[$  as follows, we obtain

$$\mathbf{y}(k) = \text{vec}(\mathbf{y}_i(k)|_{i=1}^{N_r}) = \mathbb{H}\mathbf{r}(k) + \mathbf{n}(k) \quad (12)$$

where  $\mathbb{H} = H \otimes I_M$  and  $\mathbf{n}(k) = \text{vec}(\mathbf{n}_i(k)|_{i=1}^{N_r})$  with  $\mathbf{n}_i(k) = [n_i(kT_s), n_i(kT_s+T_e), \dots, n_i(kT_s+(M-1)T_e)]^T$ . To recapitulate, a primary state model for the CPM-MIMO demodulation can be suggested, in the hidden joint state  $\mathbf{D}(k) = \text{vec}(\mathbf{D}_{L,i}(k)|_{i=1}^{N_t})$  by writing

$$\mathbf{D}(k+1) = \mathbb{F}_L \mathbf{D}(k) + \mathbf{d}(k+1) \otimes \mathbf{G}_L \quad (13)$$

$$\mathbf{y}(k) = \mathbb{H}\mathbf{r}(k) + \mathbf{n}(k) \quad (14)$$

$$= \mathbb{H}.(e^{j\mathbf{\Theta}_k} \odot e^{j2\pi h \mathbb{Q}\mathbf{D}(k)}) + \mathbf{n}(k) \quad (15)$$

where  $\mathbf{d}(k) = [d_1(k) \ d_2(k) \ \dots \ d_{N_t}(k)]^T$  denotes the vector of the transmitted symbols by the  $N_t$  antennas,  $\mathbb{F}_L = I_{N_t} \otimes F_L$ ,  $\mathbb{Q} = I_{N_t} \otimes Q$  and  $\mathbf{\Theta}_k = \boldsymbol{\theta}_k \otimes \mathbf{1}_M$  if we design by  $\boldsymbol{\theta}_k = [\theta_{k,1} \ \theta_{k,2} \ \dots \ \theta_{k,N_t}]^T$  the vector of the  $N_t$  phase states. As we can notice, the state model is related to the phase states' terms of the different CPM channels,  $e^{j\mathbf{\Theta}_k}$ , still nonlinear in the observation equation and linear state transition equation. In the following, we address the problem of the joint MAP detection of the delayed data streams  $d_i(k-k_0)|_{i=1}^{N_t}$ , when the channel matrix  $H$  is assumed to be known. Based on (13)-(15), two interesting alternatives for MIMO-CPM demodulation are proposed and discussed in the following sections.

## 5. MIMO-CPM demodulation scheme based on ML estimation of the CPM array signal

An immediate and common alternative consists in extracting the CPM signal array  $\mathbf{r}(k)$  using ML criterion as below

$$\hat{\mathbf{r}}_{ML}(k) = \arg \max_{\mathbf{r}(k)} p(\mathbf{y}(k)|\mathbf{r}(k)) \quad (16)$$

which, in case of additive gaussian noise, amounts to

$$\hat{\mathbf{r}}_{ML}(k) = \arg \min_{\mathbf{r}(k)} \|\mathbf{y}(k) - \mathbb{H}\mathbf{r}(k)\|^2 \quad (17)$$

yielding actually to

$$\hat{\mathbf{r}}_{ML}(k) = (\mathbb{H}^H\mathbb{H})^{-1}\mathbb{H}^H\mathbf{y}(k)$$

In several works, the so brought ML estimation is commonly identified as the output of a Zero Forcing (ZF) detector. Consequently, each CPM signal  $\hat{\mathbf{r}}_{i,ML}(k) = \hat{\mathbf{r}}_{ML}(k)[(i-1)M+1 : iM]$  can be extracted and passed to the CPM MAPSD-DF/differential/augmented demodulator. Hence, the obtained structure of the CPM-MIMO demodulator is based on a bank of parallel CPM decoders as explained on figure (2).

Let us note that the pre-processing of the over-sampled antenna array by the ZF block allows to decouple the demodulation procedure of the different transmitted CPM signals by eliminating the effect of the channel matrix  $\mathbb{H}$  in detriment of noise enhancement. That's why another alternative based a joint demodulation of the CPM MIMO channels is examined in the next section.

## 6. A partially joint MAP demodulation of the MIMO-CPM system

Even if the ZF pre-processing is as well as intuitive as it constitutes an efficient method to eliminate the effect of the channel which has allowed eventually the decoupling of the

different CPM channel demodulations ; we are interested here in considering a demodulation scheme based on the joint MAP detection of the delayed entries of the MIMO system as follows

$$\hat{\mathbf{d}}_{MAP}(k-L+1) = \arg \max_{\mathbf{d}(k-L+1)} p(\mathbf{d}(k-L+1)|\mathbf{y}_{0:k}) \quad (18)$$

$$\text{where } p(\mathbf{d}(k-L+1)|\mathbf{y}_{0:k}) = \sum_{\mathbf{D}(k)|\mathbf{d}(k-L+1) \in \mathbf{D}(k)} p(\mathbf{D}(k)|\mathbf{y}_{0:k}) \quad (19)$$

Here also, the hidden joint symbol state  $\mathbf{D}(k)$  takes a finite number of values, that we design by  $\mathbf{D}_j^{joint}$  for  $j = 1 \dots, N = q^{LN_r}$  and will be completely characterized by the APP vector of the same length. The joint symbol state APP vector  $\mathbf{p}^{joint}(k)$  can already be computed recursively by the MAPSD algorithm. If a decision feed-back is similarly considered to approximate the phase state vector as follows

$$\hat{\boldsymbol{\theta}}_k = \hat{\boldsymbol{\theta}}_k \otimes \mathbf{1}_M \text{ when } \hat{\boldsymbol{\theta}}_k = \hat{\boldsymbol{\theta}}_{k-1} + \pi h \hat{\mathbf{d}}_{MAP}(k-L) \quad (20)$$

$\hat{\mathbf{d}}_{MAP}(k-L)$  being the joint delayed decoded symbol sequence at instant  $k-1$  ; then the joint MAPSD-DF-based CPM-MIMO demodulation algorithm can be resumed by

1. Initialize  $\mathbf{p}^{joint}(0)$
  2. At iteration  $k$ ,  $\mathbf{p}^{joint}(k-1)$  and  $\mathbf{y}(k)$  are available at the joint CPM-MIMO MAPSD-DF
- 2.a Prediction step**

$$\mathbf{p}^{joint}(k|k-1) = \mathbb{A} \mathbf{p}^{joint}(k-1)$$

where  $\mathbb{A}$  is the probability transition matrix of the hidden Markov state  $\mathbf{D}(k)$

**2.b Filtering or updating step**

- determine the observation likelihood vector  $\mathbf{p}_n(k)$  such that

$$\mathbf{p}_n(k)[i] \propto \exp \left\{ -\frac{1}{2\sigma_n^2} \|\mathbf{y}(k) - \mathbb{H}.[e^{j\hat{\boldsymbol{\theta}}_k} \odot e^{j2\pi h \mathbb{Q} \mathbf{D}_i^{joint}}]\|^2 \right\}$$

- APP update according to  $\mathbf{p}^{joint}(k) = \frac{1}{C_k} \mathbf{p}^{joint}(k|k-1) \odot \mathbf{p}_n(k)$ ,  
where  $C_k = \mathbf{p}_n^T(k) \mathbf{p}^{joint}(k|k-1)$

**3.** multi-stream symbol detection according to (19)-(18) then  $k = k + 1$ .

As the phase states are updated separately using the last decisions on the different symbol data and not jointly, for complexity requirements, this version is designed by the partially joint CPM-MIMO MAPSD-DF demodulator. Note that an augmented version of the CPM-MIMO demodulation based on the MAPSD detection algorithm could also be implemented by including the joint phase state  $\Theta_k$  in the state to estimate as done in state model C. Here, for complexity requirements and to take benefit from the simplicity of the MAPSD detection scheme, we limit our performance investigation to the scheme operating with DF.

In the following section, the performance of the so derived partially joint CPM-MIMO MAPSD-DF and ZF-CPM-MIMO + bank of MAPSD based demodulators are studied numerically.

## 7. Numerical results

We first begin by examining the performance of the different CPM demodulation schemes based on the MAPSD. Simulation results illustrate the Bit Error Rates (BERs) using a binary CPM modulation alphabet. The modulation index is chosen such that  $h = m/P < 1$  to provide a good spectral efficiency. A smooth  $L$ -length Raised Cosine

(LRC) function is used for the shaping filter which is given by

$$g(t) = \begin{cases} \{1/(2LT_s)[1 - \cos(2\pi t/LT_s)], & \text{for } 0 \leq t \leq LT_s \\ 0 & , \text{ otherwise} \end{cases}$$

$T_s$  being the signalling period. Figure 3 shows the BER's performance of the MAPSD-differential, the MAPSD-DF and the MAPSD-augmented for different values of the partial response length  $L$ . As it is expected, the MAPSD-differential version performs poorly compared to the MAPSD-DF and the MAPSD-augmented due to noise amplification (around 6 dB gain is achieved at BER of  $10^{-2}$ ), even if it constitutes an adequate alternative for noncoherent CPM demodulation. Similar good BER's performance are actually depicted on both figures 3 and 6 for both the MAPSD-DF and the MAPSD-augmented. This shows a certain robustness of the MAPSD-DF towards the phase state  $\theta_k$  deduced through processing iterations by a DF mechanism. This robustness can be already explained by the use of the  $L^{th}$  delayed symbol in the DF and the nonlinear saturation of the  $\theta_k$  contribution through the exponential. This recommends clearly then the use of the MAPSD-DF rather than the augmented one since the complexity (evaluated in parallel treatments) will be divided by  $P$  or  $2P$ ; besides the fact that it doesn't need a fractional value of the modulation index. The MAPSD-detection is then enhanced by increasing the up-sampling factor  $M$  for those same versions based on state models A and C (see figure 6). In fact, both the MAPSD-DF and the MAPSD-augmented are basically Bayesian detectors performing implicitly a classification of the so processed observation, namely the up-sampled noisy modulated CPM signal. So, their performance depends on its ability to separate the different observation classes corresponding to each possible value of the delayed symbol. Figure 7 illustrates, in this aim, the normalized histogram of the quantity  $DISP = \text{norm}(p(d(k-L+1) = +1|\mathbf{z}_{0:k}) - p(d(k-L+1) = -1|\mathbf{z}_{0:k}))$  for  $M = 2, 4$  and 8 using the MAPSD-DF demodulation scheme. Note that the distribution of  $DISP$  becomes

picked around values towards 1 by increasing  $M$  ; the presence of values of  $DISP$  around 0.1 and 0.2 indicates a poor separability of the classes which induces more errors at the decision stage.

For the MIMO system, chosen as a synchronous one, a Rayleigh bloc fading channel is simulated with  $h_{ij}$  assumed to be a zero-mean complex gaussian variable with normalized variance. The channel matrix  $H$  is varied each bloc of 100 binary symbols. The following parameters are chosen for the  $N_t$  CPM modulators :  $L = 3$ ,  $h = 1/4$  and  $M = 8$ . Figure 8 depicts the averaged BERs of the  $N_t$  data entries versus SNR. So, the obtained results for both the so-suggested Bayesian CPM-MIMO demodulators are concordant with a performance enhancement when increasing the number of receive antennas. As also expected, the partially joint CPM-MIMO MAPSD based demodulator using the joint DF outperforms the ZF-CPM-MIMO + bank of MAPSD-DF since the intermediate ZF processing introduces a breaking point within the optimal MAP joint symbol detection scheme of  $\mathbf{D}(k)$  and since the joint estimation of the correlated data entries via the MIMO channel should yield inherently to better estimates than considering each decoding scheme separately. This fact is illustrated by figure 9 on which we can see that that the version of the partially CPM-MIMO based MAPSD with true DF or DF computed according to (20) outperforms that of the CPM-MIMO-ZF + bank of MAPSD-DF even when a true DF is used.

## 8. Conclusion

In this work, CPM demodulation is revisited at first, through the suggestion of multiple state model descriptions of the problem and the corresponding Bayesian demodulation schemes built around the MAPSD algorithm are presented. Moreover, two new optimal MAP CPM-MIMO symbol-by-symbol detectors, derived using a state model description of the MIMO channel demodulation problem, are proposed. The corresponding Bayesian

detection algorithms consist actually in different MAPSD demodulation schemes ; presenting then a noteworthy implementation simplicity as well as an acceptable complexity. Particularly, the version of the partially joint CPM-MIMO MAPSD-DF demodulator presents enhanced BER's performance compared to the one operating with ZF pre-processing and structured into a bank of MAPSD/DF CPM demodulators. An imminent alternative to this work will address the problem of developing a coupled Bayesian MIMO channel estimator to the CPM demodulator.

## References

- [1] R. Amara Boujema. *A suitable state formulation of the CPM demodulation problem for several optimal Bayesian tracking filters* . 2nd International Conference on Signals, Circuits and Systems, Hammamet, November 2008.
- [2] J.G. Proakis. *Digital communications*. McGraw Hill series. Third edition (1995). New York.
- [3] J. Tan, G.L. Stuber. *Frequency-domain equalization for continuous phase modulation*. IEEE Trans. on wireless communications, vol. 4, No. 5, September 2005
- [4] M.P. Wylie-Green, E.S. Perrins. *A generalized CPM-SC-FDMA transmission scheme suitable for future aeronautical telemetry*. IEEE Military Communications Conference(MILCOM) 2008
- [5] H. Nguyen, B.C. Levy. *Blind and semi-blind equalization of CPM signals with the EMV algorithm*. IEEE Trans. on signal processing, vol. 51, No. 10, pp. 2650-2664, October 2003.

- [6] J.C.S Cheung, R. Steele. *Soft-decision feedback equalizer for continuous phase modulated signals in wideband mobile radio channels*. IEEE Transactions on communications, vol. 42, No. 2/3/4, february/March/April, 1994.
- [7] J.P. Foneska. *Soft-decision phase detection with Viterbi decoding for CPM signals*. IEEE Trans. on communications, vol.47, No. 12, December 1999.
- [8] P.A. Murphy, G.E. Ford. *Cochannel receivers for CPM signals based upon the Laurent representation*. Tech. Symposium on Wireless Personal communications, Virginia, 1996
- [9] P.A. Murphy, M. Golanbari, G.E. Ford, M.J. Ready. *Optimum and reduced complexity multiuser detectors for asynchronous CPM signalling*. IEEE Transactions on wireless communications, vol.5, No.8, August 2006.
- [10] P.A. Murphy, G.E. Ford, M. Golanbari. *MAP Symbol detection of CPM bursts*. Proceedings of the tech. Symposium on wireless personal communications, Virginia, 1997.
- [11] M.J. Gertsman, J.H. Lodge. *symbol-by-Symbol MAP demodulation of CPM and PSK signals on Rayleigh flat-fading channels*. IEEE Trans. on communications, vol. 45, No. 7, July 1997
- [12] R. Balasubramanian, M.P. Fitz. *Soft-output detection of CPM signals in frequency, flat fading channels*. IEEE journal on selected areas in communications, vol. 18, No. 7, July 2000.
- [13] R. Balasubramanian, M.P. Fitz, J.V. Krogmeier. *Optimal and suboptimal symbol-by-symbol demodulation of continuous phase modulated signals*, IEEE Trans. on communications, vol. 46, No. 12, pp. 1662-1668, December 1998.

- [14] Q. Zhao, H. Kim, G.L. Stuber. *Innovations-based MAP estimation with application to phase synchronisation for serially concatenated CPM*. IEEE Trans. on wireless communications, vol .5, No. 5, May 2006
- [15] X. Zhang, M.P. Fitz. *Symmetric information rate for continuous phase channel and BLAST architecture with CPM MIMO system*. IEEE International conference on communications, May 2003
- [16] W. Zhao, G.B. Giannakis. *Reduced complexiy receivers for layered space-time CPM*. IEEE Trans. on wireless communications, vol.4, No. 2, pp. 574-582, March 2005.
- [17] O. Weikert, U. Zolzer. *A Layered MIMO CPM System with Incoherent Demodulation*. IEEE International Conference on Signal Processing and Communications (IC-SPC 2007), Nov. 2007.
- [18] A.H. Jaswinski. *Stochastic processes and filtering theory*. Academic Press, 1970, NY.
- [19] H. Tanizaki. *Nonlinear filters : estimation and applications*. Second edition. 1996.
- [20] R. Amara, S. Marcos. *Parallel Kalman filtering for optimal symbol-by-symbol estimation in an equalization context*, Signal Processing, ELSEVIER, Vol. 85, Issue 6, pp. 1125-1138, June 2005
- [21] R. Chen, X. Wang, J.S. Liu. *Adaptive joint detection and decoding in flat-fading channels via mixture Kalman filtering*. IEEE Transactions on information theory, vol. 46, No. 6, pp. 2079-2094, September 2000
- [22] R. Amara, S. Marcos. *A network of Kalman filters for MAP symbol-by-symbol equalization*. Proc. ICASSP, vol. 5, pp. 2697-2700, Istambul, 2000.

- [23] I.B. collings, J.B. Moore. *An adaptive hidden Markov model approach to FM and M-ary DPSK demodulation in noisy fading channels*. Signal Processing, Vol. 47, Issue 1, pp. 7184, November 1995.
- [24] I. B. Collings, J. B. Moore. *An HMM approach to adaptive demodulation of QAM signals in fading channels*. International Journal of Adaptive Control and Signal Processing, Vol. 8, Issue 5, pp. 457-474, September/October 1994.
- [25] M. Bellanger. *An adaptive equalizer for frequency modulated signals*. First International Symposium on Control, Communications and Signal Processing (ISCCSP), 2004.
- [26] H. Mathis. *Differential detection of GMSK signals Low  $B_rT$  using the SOVA*. IEEE trans. on communications, vol.46, No.4, April 1998.
- [27] X. Huang, Y. Li. *Simple noncoherent CPM receivers by PAM decomposition and MMSE equalization*. the 14<sup>th</sup> PIMRC communication proceedings, 2003.
- [28] P Moqvist, TM Aulin. *Orthogonalization by principal components applied to CPM*. IEEE Transactions on Communications, Nov. 2003.
- [29] M. Xiao and T. Aulin. *Serially Concatenated Continuous Phase Modulation with Ring Convolution Codes*, IEEE Transactions on Communications, August 2006, pp. 1387-1396.
- [30] M. Xiao and T. Aulin. *Irregular Repeat Continuous Phase Modulation*, IEEE Communication Letters, August, 2005.

SNR	-4	-2	0	2	4	6	8	10
$\sigma_{n'}^2$	2.5119	1.5849	1	0.6310	0.3981	0.2512	0.1585	0.1
$\hat{\sigma}_{n'}^2$	2.5127	1.5854	1.0003	0.6312	0.3982	0.2513	0.1585	0.1
$\sigma_{n''}^2$	11.3333	5.6817	3	1.66	0.9547	0.5655	0.3421	0.21
$\hat{\sigma}_{n''}^2$	11.3354	5.6815	2.9995	1.6596	0.9545	0.5654	0.3421	0.21

Table 1: Theoretical and sample variances of  $n'$  and  $n''$

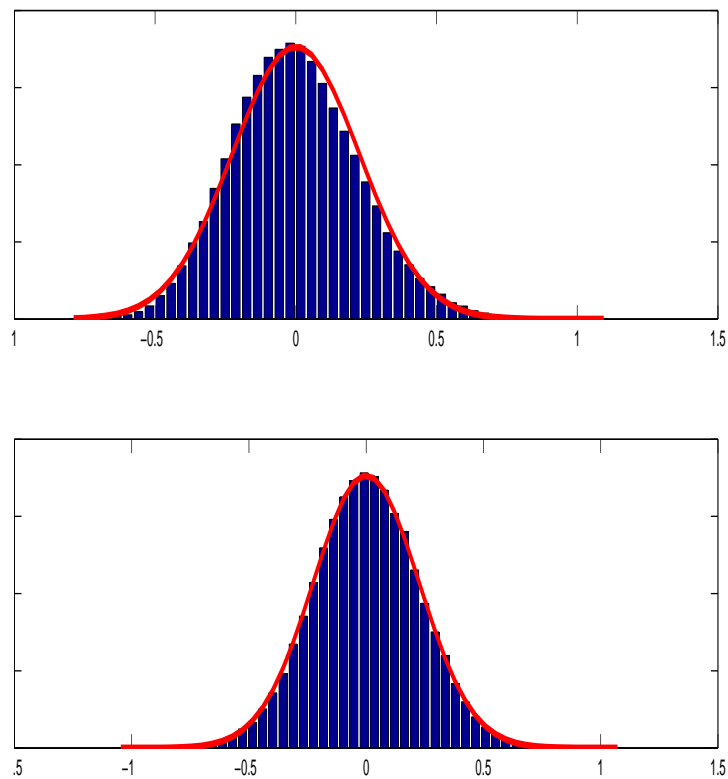


Figure 1: Sample and theoretical pdf of the real and imaginary parts of the noise  $n''(\cdot)$  for  $\sigma_n^2 = 0.05$ ,  $L = 3$ ,  $M = 8$  and  $h = 1/4$

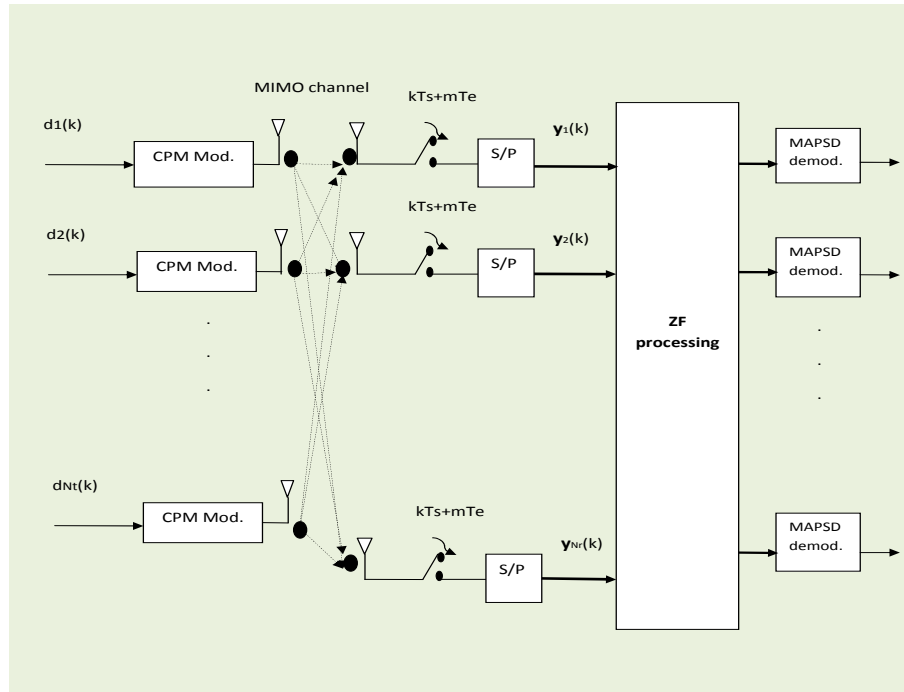


Figure 2: Scheme of the ZF-CPM-MIMO + bank of MAPSD demodulators

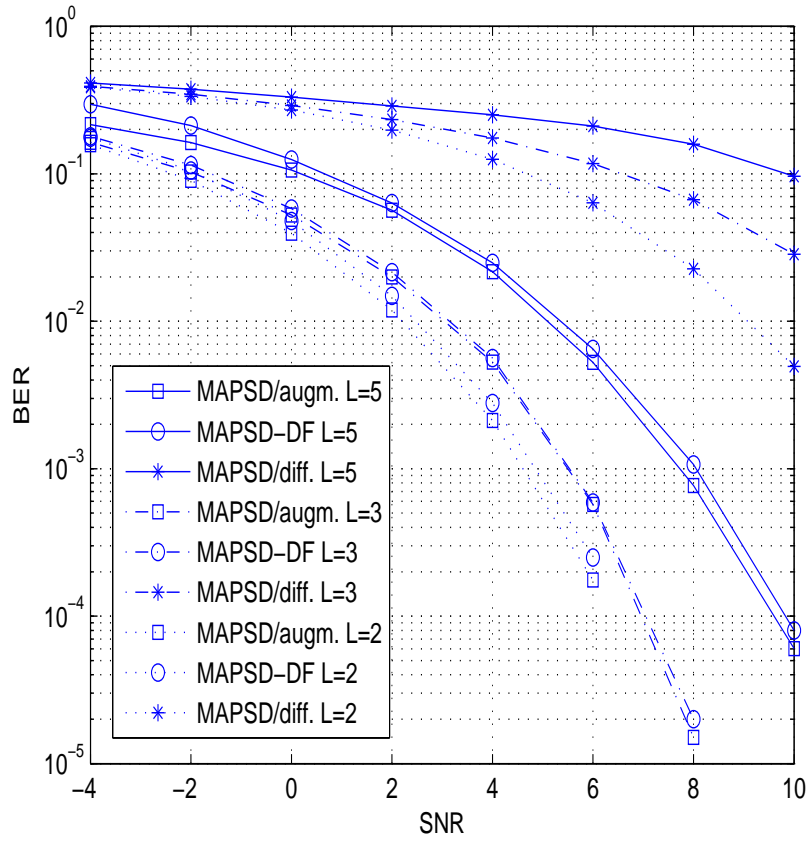


Figure 3: BER's performance for the MAPSD-differential, the MAPSD-DF and the MAPSD/augmented for different values of the partial response length  $L$  and for  $M = 8$ ,  $h = 1/5$

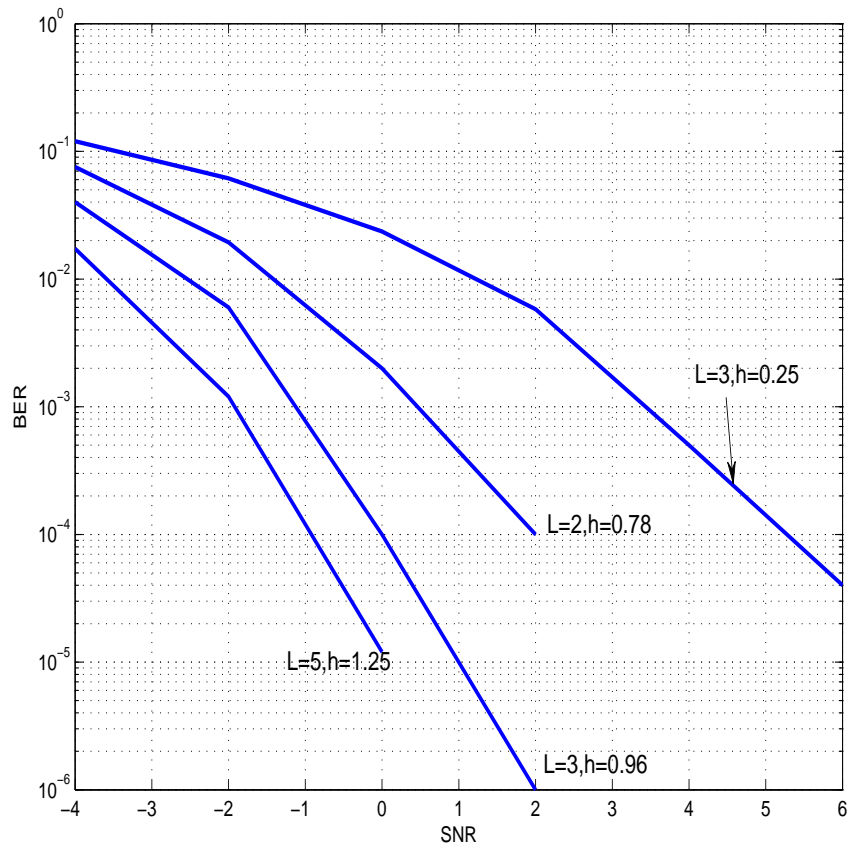


Figure 4: BER's performance for the MAPSD-DF for different values of  $h$  and for  $M = 8$

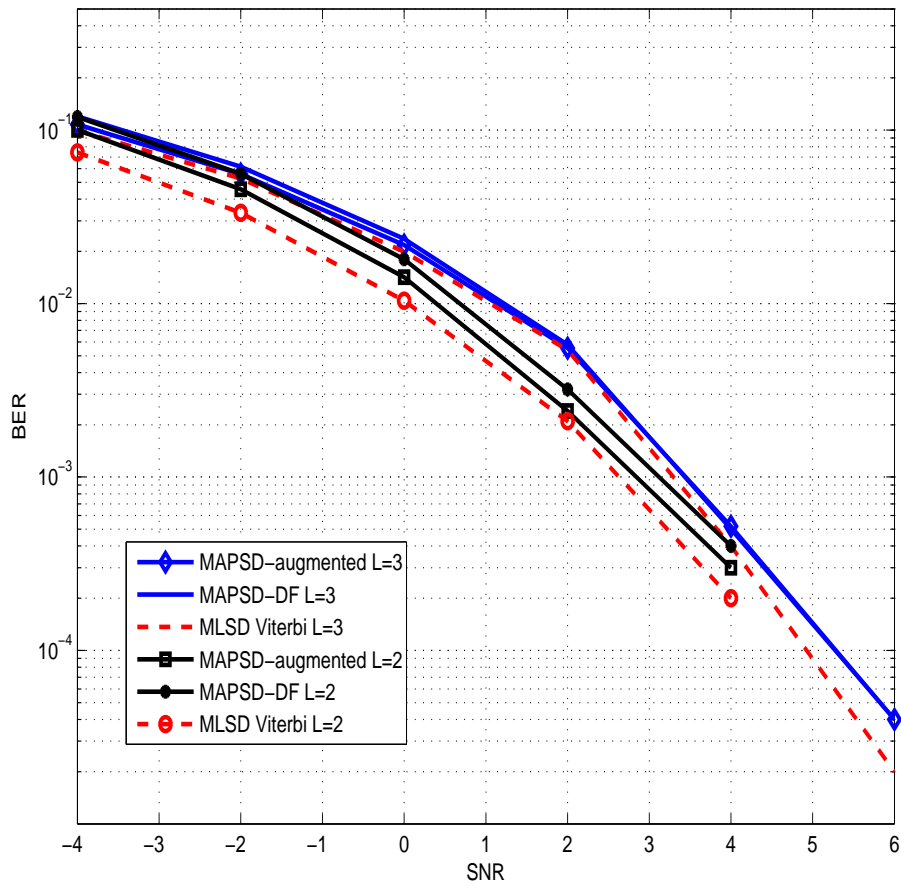


Figure 5: BER's performance for the MAPSD-DF, the MAPSD-augmented and the Viterbi-based MLSD CPM decoders,  $M = 8$ ,  $h = 1/4$

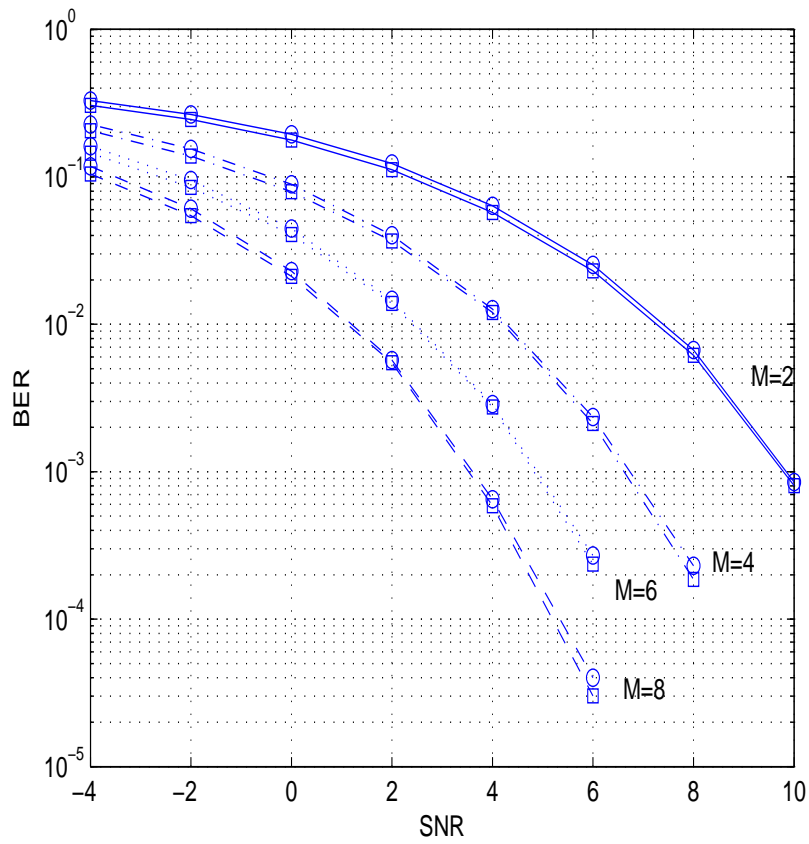


Figure 6: Effect of the upsampling factor  $M$  on the BER's performance of the MAPSD-DF 'o' and the MAPSD/augmented '□',  $h = 1/4$ ,  $L = 3$

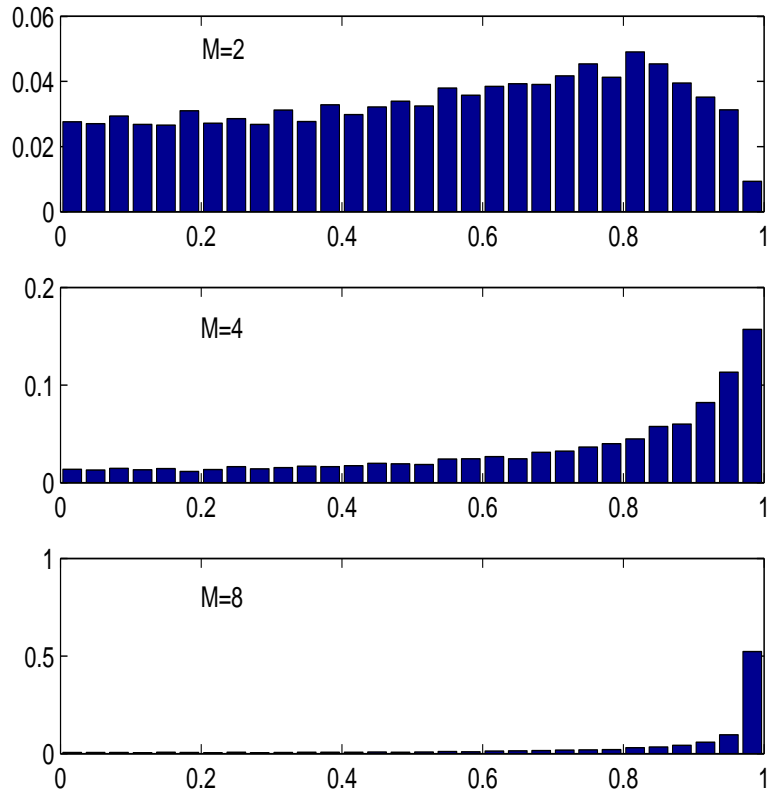


Figure 7: Normalized histogram of  $DIS P$ ,  $M = 8$ ,  $L = 3$  and  $h = 1/4$

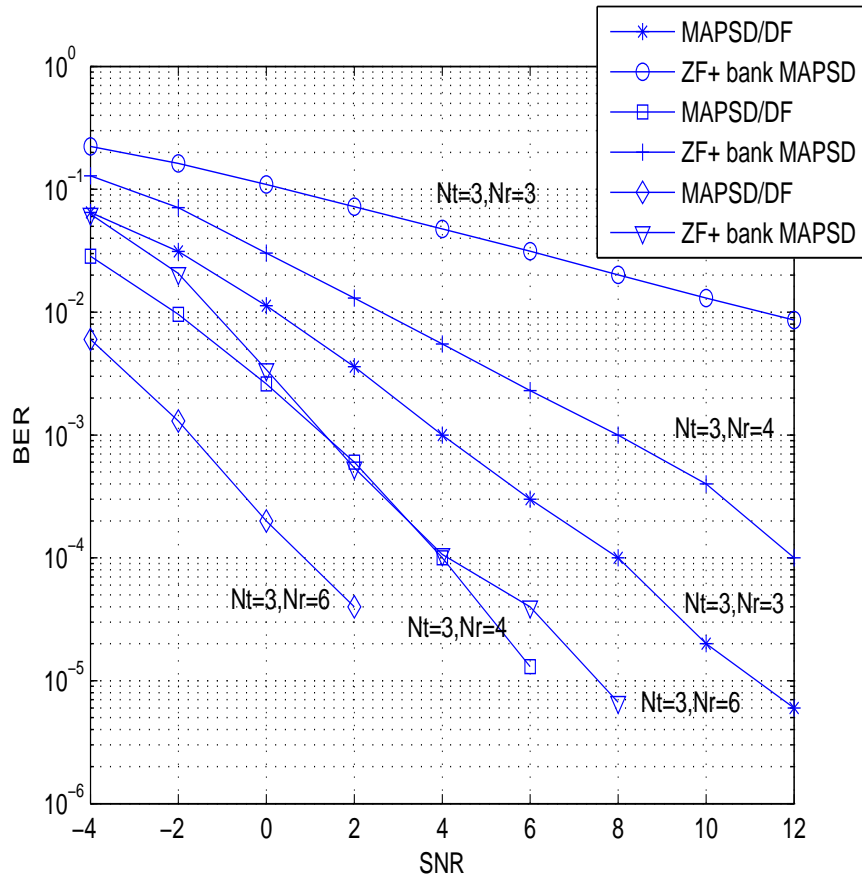


Figure 8: Performance of the CPM-MIMO MAPSD-DF and the ZF-CPM-MIMO + bank of MAPSD-DF based demodulators as function of  $N_t$  and  $N_r$ ,  $M = 8$ ,  $L = 3$ ,  $h = 1/4$ , the channel matrix  $H$  is varied each 100 sampling iterations

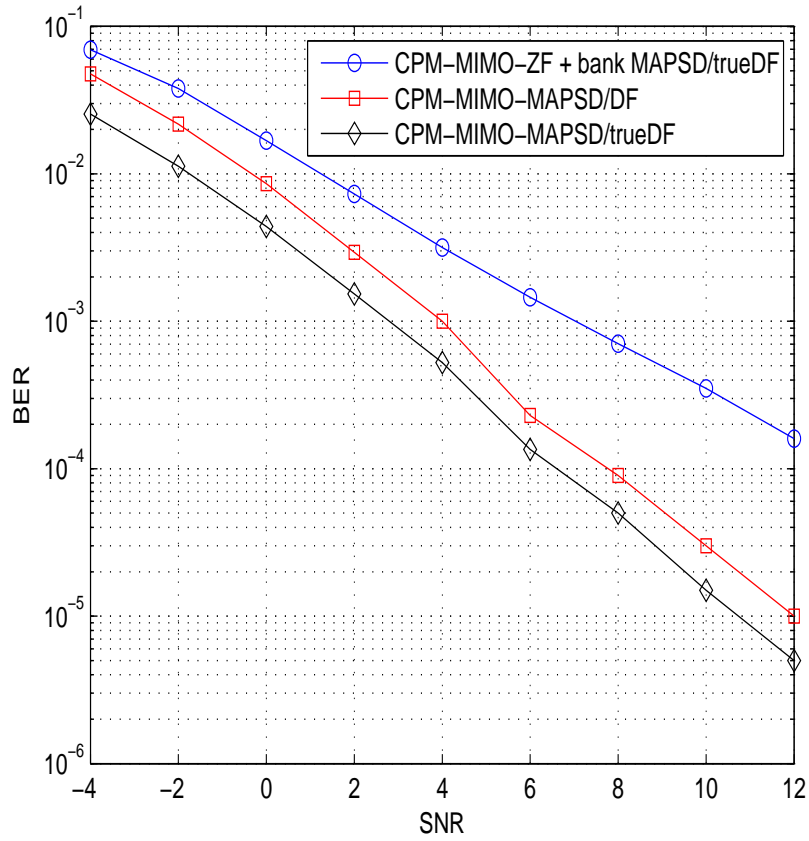


Figure 9: Effect of the DF on both proposed CPM-MIMO Bayesian demodulators,  $N_t = 2$  and  $N_r = 3$ ,  $M = 8$ ,  $L = 3$  and  $h = 1/4$